Electronic Supplementary Information

A promising dual mode SPECT/CT imaging platform based on ^{99m}Tc-labeled multifunctional dendrimer-entrapped gold nanoparticles

Shihui Wen,[a,b]† Lingzhou Zhao,[c]† Qinghua Zhao,[d] Du Li,[a] Changcun Liu,[c] Zhibo Yu,[b] Mingwu Shen,[b] Jean-Pierre Majoral[e], Serge Mignani[f], Jinhua Zhao,*[c] and Xiangyang Shi*[a,b]

[a] State Key Laboratory for Modification of Chemical Fibers and Polymer Materials, Donghua University, Shanghai 201620, People's Republic of China

[b] College of Chemistry, Chemical Engineering and Biotechnology, Donghua University, Shanghai 201620, People's Republic of China

[c] Department of Nuclear Medicine, Shanghai General Hospital, School of Medicine, Shanghai Jiaotong University, Shanghai 200080, People's Republic of China

[d] Department of Orthopaedics, Shanghai General Hospital, School of Medicine, Shanghai Jiaotong University, Shanghai 200080, People's Republic of China

[e] Laboratoire de Chimie de Coordination du CNRS, 205 route de Narbonne F-31077 Toulouse cedex 4, France

[f] Université Paris Descartes, PRES Sorbonne Paris Cité, CNRS UMR 860, Laboratoire de Chimie et de Biochimie Pharmacologiques et Toxicologique, 45, rue des Saints Pères, 75006 Paris, France

---

* Corresponding author. E-mail: xshi@dhu.edu.cn (X. Shi) and Zhaojinhua1963@126.com (J. Zhao).

† Authors contributed equally to this work.

Experimental Section

Materials. G5.NH_2 dendrimers were purchased from Dendritech (Midland, MI). Glycidol, cDTPAA, stannous chlorides ($SnCl_2$), and 3-(4,5-dimethylthiazol-2-yl)-2,5-diphenyltetrazolium bromide (MTT) were purchased from Aldrich (St. Louis, MO). PEG monomethyl ether with one end of carboxyl group (*m*PEG-COOH, Mw = 5 000) was from Shanghai Yanyi Biotechnology Corporation (Shanghai, China). Sodium borohydride ($NaBH_4$) and 1-ethyl-3-(3-dimethylaminopropyl)carbodiimide hydrochloride (EDC) were purchased from J&K Chemical Ltd. (Shanghai, China). ^{99m}Tc-pertechnetate was supplied by Shanghai GMS Pharmaceutical Co., Ltd. (Shanghai, China). SKOV-3 cells (a human ovarian carcinoma cell line) were obtained from Institute of Biochemistry and Cell Biology (the Chinese Academy of Sciences, Shanghai, China). RPMI 1640 medium, fetal bovine serum (FBS), penicillin, and streptomycin were purchased from HyClone Lab., Inc. (Logan, UT). $HAuCl_4 \cdot 4H_2O$, acetic anhydride (Ac_2O), triethylamine (TEA), and all other chemicals and solvents were from Sinopharm Chemical Reagent Co., Ltd. (Shanghai, China). Cellulose dialysis membranes (molecular weight cut-off, MWCO = 8 000-14 000) were acquired from Shanghai Yuanye Biotechnology Co., Ltd. (Shanghai, China). Disposable PD-10 desalting columns were procured from GE Pharmacia (Shanghai, China).

Surface Modification of G5.NH_2 with cDTPAA and *m*PEG-COOH. G5.NH_2 (20.0 mg) dissolved in water (15 mL) was reacted with cDTPAA (1.1 mg/mL, in 2 mL water) under vigorous magnetic stirring at room temperature. The reaction was stopped after 8 h to get G5.NH_2-DTPA as crude product, which was used in the next step without further purification. In a parallel experiment, *m*PEG-COOH (76.9 mg) was dissolved in 10 mL water with 20 molar equivalents of G5.NH_2, and reacted with EDC (7.69 mg/mL, in 5 mL water) under vigorous magnetic stirring for 3 h. The EDC-activated *m*PEG-COOH was then added dropwise into an aqueous solution of the raw product of G5.NH_2-DTPA under magnetic stirring at room temperature. The reaction was continued for 2 days

to obtain G5.NH_2-DTPA-*m*PEG conjugates as a crude product, which was used in the next step without any further purification step.

Synthesis of Au DENPs. The synthesized G5.NH_2-DTPA-*m*PEG conjugates were used as templates to entrap Au NPs. The procedure to synthesize Au DENPs was adopted from that reported in our previous study[1] with the dendrimer/Au salt molar ratio at 1:200. Briefly, an $HAuCl_4$ solution (30 mg/mL, in 2.1 mL water) was added to the above G5.NH_2-DTPA-*m*PEG solution under vigorous stirring at room temperature. After 30 min, an icy cold $NaBH_4$ solution (10.0 mg/mL, in 2.8 mL water) was added dropwise to the Au salt/dendrimer mixture under vigorous stirring, which led to the formation of Au DENPs. The Au DENPs were prepared in parallel. For acetylated product, 2 h later, the Au DENP solution was added with TEA (78.0 μL) and the solution was thoroughly mixed for 30 min, followed by addition of Ac_2O (42.0 μL) under vigorous magnetic stirring for 24 h at room temperature. For hydroxylated product, 2 h later, the Au DENP solution was added with glycidol (84.0 μL) under vigorous magnetic stirring for 24 h at room temperature. The reaction mixture of either acetylated or hydroxylated product was subjected to extensive dialysis against phosphate buffered saline (PBS, 3 times, 2 L) and water (5 times, 2 L) for 3 days to remove the excess of reactants and byproducts. Followed by a lyophilization process, $\{(Au^0)_{200}$-G5.NHAc-DTPA-*m*PEG$\}$ DENPs (Au-Ac DENPs) or $\{(Au^0)_{200}$-G5.NGlyOH-DTPA-*m*PEG$\}$ DENPs (Au-Gly DENPs) were obtained. The intermediate products of G5.NH_2-DTPA and G5.NH_2-DTPA-*m*PEG were also collected and purified in order to analyze the number of DTPA and PEG moieties attached onto each G5 dendrimer.

^{99m}Tc was labeled onto the surface of Au DENPs *via* the DTPA ligands according to the literature.[2] In a typical experiment, Au-Ac DENPs (200 μg) and $SnCl_2$ (50 μg) were added to a 5 mL vial containing 250 μL PBS (pH = 7.4), and sterile ^{99m}Tc-pertechnetate (740 MBq, 1 mL) was added to the vial immediately with stirring. After incubation at room temperature for 30 min, PD-10 desalting

columns were used to purify the ^{99m}Tc-Au-Ac DENPs. For the synthesis of ^{99m}Tc-Au-Gly DENPs, the experiment was carried out in the same way as described above.

Characterization Techniques. ^{1}H NMR spectra were collected using a Bruker DRX 400 nuclear magnetic resonance spectrometer. Samples were dissolved in D_2O before experiments. UV-vis spectra were recorded by a Lambda 25 UV-vis spectrophotometer (Perkin Elmer, Waltham, MA). Samples were dissolved in water before measurements. The size and morphology of the formed Au DENPs were characterized by a JEOL 2010F analytical electron microscope (JEOL, Tokyo, Japan) operating at 200 kV. The Au composition of the formed Au DENPs was determined by Leeman Prodigy inductively coupled plasma-optical emission spectroscopy (ICP-OES, Hudson, NH). Dynamic light scattering (DLS) and zeta potential measurements were performed using a Malvern Zetasizer Nano ZS model ZEN3600 (Worcestershire, UK) equipped with a standard 633 nm laser. To examine the X-ray attenuation property, solutions of the formed Au DENPs and Omnipaque (iohexol 300, GE Healthcare) with different Au or I concentrations were prepared. CT scans were performed using a GE LightSpeed VCT imaging system (GE Medical Systems, Milwaukee, WI) with 100 kV, 220 mA, and a slice thickness of 1.25 mm. Contrast enhancement was evaluated in Hounsfield units (HU) for each concentration of the formed Au DENPs or Omnipaque.

Radiochemical Purity. The radiochemical purity of ^{99m}Tc-Au-Ac DENPs and ^{99m}Tc-Au-Gly DENPs was tested by instant thin-layer chromatography (ITLC) using silica gel-coated fiber glass sheets (Macherey-Nagel, GmbH & Co. KG, Düren, Germany) and saline as the mobile phase. The sheets were scanned and analyzed by Thin-Layer Chromatogram Scanner (Bioscan Inc., Tucson, AZ). The radioactive contaminants, such as reduced/hydrolyzed ^{99m}Tc and free ^{99m}Tc-pertechnetate, migrated in the thin-layer column, while the labeled product remained at the starting point. The optimum labeling yield (95%) was achieved at room temperature for 30 min when 50 μg of $SnCl_2$ was

used in the presence of 200 μg of Au-Ac DENPs or Au-Gly DENPs and 740 MBq of ^{99m}Tc-pertechnetate. Quality control tests showed that both ^{99m}Tc-Au DENPs contained less than 5% free ^{99m}Tc-pertechnetate or reduced/hydrolyzed ^{99m}Tc.

***In Vitro* Radiostability Study.** To examine the *in vitro* radiostability of the product in saline (at room temperature) and serum (at 37 °C), ^{99m}Tc-Au-Ac DENPs or ^{99m}Tc-Au-Gly DENPs (200 μL, 1 mg/mL) were mixed with 2 mL of saline (0.9%) or serum. ITLC was carried out to assess the radiochemical purity after the particles were incubated for 5 min, 1 h, 2 h, and 6 h, respectively.

Hemolysis Assay. For hemolysis study, fresh human blood stabilized with citrate was provided by Shanghai General Hospital (Shanghai, China) after approval by the ethical committee of Shanghai General Hospital. Healthy red blood cells (RBCs) were collected according to the procedures described in the literature.[3] Briefly, RBCs were separated from 1 mL of fresh blood by centrifugation (3 000 rpm, 3 min) and washed with 6 mL of PBS for 4 times. Then, the obtained RBCs were diluted 10 times with PBS. Thereafter, 0.1 mL of the diluted RBC suspension was added to a 2.0-mL tube prefilled with 0.9 mL of water (positive control), 0.9 mL of PBS (negative control), or 0.9 mL of PBS containing Au-Ac DENPs or Au-Gly DENPs with different concentrations (50, 100, 200, or 400 μg/mL), respectively. In the same time, 0.1 mL of PBS was added to 0.9 mL of PBS containing Au-Ac DENPs or Au-Gly DENPs with the same concentrations as the blank controls. The mixtures were left to stand for 2 h at room temperature and centrifuged at 10 000 rpm for 1 min. Finally, the absorbance of the supernatants was measured by UV-vis spectrophotometer and the hemolysis percentages of the samples were calculated according to the following equation:

$$\text{Hemolysis percentage} = (A_s - A_{bc} - A_{nc})/(A_{pc} - A_{nc}) \times 100\% \quad (1)$$

where A_s is the absorbance of the samples at 541 nm, A_{bc}, A_{nc}, and A_{pc} are the absorbances of the

blank, negative, and positive controls at 541 nm, respectively.

***In Vitro* Cytotoxicity Assay.** SKOV-3 cells were cultured in a 37 ^{o}C incubator with 5% CO_2 in RPMI 1640 cell culture medium supplemented with 100 μg/mL streptomycin, 100 U/mL penicillin, and 10% FBS. The cytotoxicity of the Au DENPs was evaluated by MTT cell viability assay. SKOV-3 cells were seeded into a 96-well plate at a density of 8 000 cells per well and incubated in regular RPMI 1640 medium for 24 h. Subsequently, the medium was replaced with fresh medium containing Au-Ac DENPs or Au-Gly DENPs at different Au concentrations (0, 2.5, 5, 10, 20, 40, or 80 μM, respectively). After 24 h incubation, MTT (5 mg/mL, 20 μL in PBS) was added to each well and the cells were incubated continually for another 4 h. Thereafter, the medium was carefully removed, followed by the addition of DMSO (200 μL) to dissolve the formazan crystals. Finally, the absorbance at a wavelength of 570 nm in each well was recorded using a Multiskan MK3 ELISA reader (Thermo Scientific, Waltham, MA). Data were presented as mean ± standard deviation (SD) of the triplicate wells for each sample.

***In Vivo* Toxicity and Histology Analysis.** All animal studies were carried out according to the standard protocols approved by the ethical committee of Shanghai General Hospital for animal care. For *in vivo* toxicity studies, male 5-week-old ICR mice (23-25 g, Sino-British SIPPR/BK Lab Animal Ltd., Shanghai, China) were used. The body weights of ICR mice both in the test groups and control group (n = 4 for each group) were recorded for one month after administration. For the test groups, Au-Ac DENPs or Au-Gly DENPs ([Au] = 0.08 M, 0.20 mL in saline solution) were intravenously injected *via* the tail vein. ICR mice injected with saline (0.20 mL) were used as the control. In terms of histology studies, the above ICR mice were sacrificed at one month post administration of the particles and the major organs including heart, liver, spleen, lung, and kidney were harvested. Then, the organs were fixed in 10% neutral buffered formalin, embedded

in paraffin, and sectioned with a thickness of 3 μm, followed by staining with H&E (hematoxylin and eosin). After that, the histological sections were observed using a Leica DM IL LED phase contrast microscope.

***In Vivo* Micro-SPECT/CT Imaging.** Firstly, ICR mice were anesthetized through intraperitoneal injection of pentobarbital sodium (40 mg/kg). Then, ^{99m}Tc-Au-Ac DENPs or ^{99m}Tc-Au-Gly DENPs ([^{99m}Tc] = 370 MBq/mL, [Au] = 0.08 M, in 0.20 mL saline) were intravenously injected to the mice. SPECT/CT scans were performed at 0.5, 1, and 2 h postinjection by NanoSPECT/CT In Vivo Animal Imager (Bioscan Inc., Tucson, AZ). During SPECT/CT imaging, mice were anesthetized using isoflurane (2%) through a mask. All imaging data were reconstructed and analyzed by an InVivo Scope software (Bioscan, Inc., Tucson, AZ).

***In Vivo* Biodistribution.** The ICR mice (23-25 g) were used for biodistribution studies of the ^{99m}Tc-Au-Ac DENPs or ^{99m}Tc-Au-Gly DENPs. After intravenous injection ([^{99m}Tc] = 370 MBq/mL, [Au] = 0.08 M, 0.20 mL in saline), the mice were euthanized at 1, 2, 4, or 12 h postinjection. The blood, muscle, and major organs were collected and weighed, followed by radioactivity measurement through a well-type gamma spectrometer and count/min values were decay corrected. Results were presented as the percentage of injected dose/gram (%ID/g) of wet tissue and shown as mean ± SD (n = 4) for each group.

For long term *in vivo* biodistribution studies, the ICR mice were intravenously injected with the Au-Ac DENPs or Au-Gly DENPs ([Au]= 0.08 M, 0.20 mL in saline). At 48, 96, and 168 h postinjection, the mice were euthanized. The blood, muscle, and major organs were harvested, weighed, and digested by aqua regia solution. ICP-OES analysis was perfomed to measure the Au content in each tissue or organ.

Blood Analysis. For serum biochemistry assay and hematology analysis, healthy ICR mice were intravenously injected with Au-Ac DENPs or Au-Gly DENPs ([Au] = 0.08 M, 0.20 mL in saline). In the same time, other 4 healthy ICR mice injected with saline (0.20 mL) were used as control. The blood drawing from eyeball of mice was harvested and collected at 30 days postinjection. Then, serum biochemistry parameters (aspartate aminotransferase (AST), alkaline phosphatase (ALP), alanine aminotransferase (ALT), blood urea nitrogen levels (BUN), and the ratio of albumin and globulin (A/G)) and hematology parameters (hemoglobin (HGB), white blood cell (WBC), red blood cell (RBC), hematocrit (HCT) and platelet count (PLT)) were analyzed. Data were presented as mean ± SD (n = 4) for each group.

***In Vivo* SPECT/CT Lymph Node Imaging.** For SPECT/CT lymph node imaging, male New Zealand white rabbits (1.5 kg, Sino-British SIPPR/BK Lab Animal Ltd., Shanghai, China) were anesthetized through intraperitoneal injection of pentobarbital sodium (40 mg/kg). Then, ^{99m}Tc-Au-Ac DENPs or ^{99m}Tc-Au-Gly DENPs ([Au] = 0.08 M, [^{99m}Tc] = 370 MBq/mL, 0.50 mL in saline) were injected intradermally into the left and right paws of the rabbit, respectively. SPECT imaging was performed at 1, 2, and 4 h postinjection by an Infinia SPECT scanner equipped with an Xeleris Workstation and Low Energy General Purpose collimator (GE Medical Systems), while CT scans were performed at the same time points by a GE Discovery STE PET/CT system with a tube voltage of 100 kV, an electrical current of 220 mA, and a slice thickness of 1.25 mm. Reconstructed 3D images were obtained using GE Advantage Workstation AW4.3.

Part of Results and Discussion

Synthesis and Characterization of Functionalized Au DENPs. DTPA-conjugated G5 dendrimer was characterized by ^{1}H NMR. Because the -CH_2- proton signals of DTPA overlap with

those of the ethylene backbone of PAMAM dendrimers, the number of DTPA ligands attached onto each G5 dendrimer was calculated to be 7.6 using an indirect method.[1] The calculated number is quite similar to the theoretical value of 8.0 based on the initial molar feeding ratio. In addition, zeta potentials of G5.NH_2 and G5.NH_2-DTPA dendrimers were measured to confirm the surface modification. Clearly, the positive surface potential of G5.NH_2 (36.3 ± 5.6 mV) decreases to 25.5 ± 6.1 mV after the cDTPAA modification.

Surface PEGylation is demonstrated to be one of the most preferred and effective methods to improve the biocompatibility of NPs, to alleviate clearance of NPs by the reticuloendothelial system (RES), and to extend the blood circulation time of NPs.[4-7] In this study, we modified G5.NH_2-DTPA dendrimers with *m*PEG-COOH *via* EDC chemistry. By integration of the related NMR peaks (Figure S1, Supporting Information), we were able to estimate the number of *m*PEG moieties onto each G5 dendrimer to be 17.6. Due to the covered amine group, PEGylation led to a significantly decreased surface potential of the dendrimers (18.3 ± 4.3 mV for G5.NH_2-DTPA-*m*PEG) when compared to those before PEGylation (25.5 ± 6.1 mV for G5.NH_2-DTPA).

The final formed Au DENPs were exhaustively characterized by zeta-potential measurements, ^{1}H NMR, TEM, and UV-vis spectrometry, respectively. The Au-Ac DENPs and Au-Gly DENPs have a surface potential of 1.9 ± 1.8 and 2.3 ± 0.9 mV, respectively, suggesting successful surface acetylation or hydroxylation. This can be further confirmed by ^{1}H NMR (Figure S1c and S1d), similar to our previous reports.[8, 9] TEM images reveal that the Au core NPs for both Au-Ac DENPs and Au-Gly DENPs possess a close-to-spherical shape with quite a uniform size distribution (Figures 2a and 2e), and the mean diameters of the Au core NPs are 3.3 and 3.2 nm, respectively for the Au-Ac DENPs and Au-Gly DENPs (Figures 2b and 2f). High-resolution TEM images show that the Au core NPs for both the Au-Ac DENPs and Au-Gly DENPs are crystalline, as lattices of Au crystals can be clearly observed (insets of Figures 2a and 2e). Their crystalline nature was also confirmed using selected area electron diffraction (SAED), where the (111), (200), (220) and (311) rings can be used to prove the face-centered-cubic crystal structure of both Au NPs (Figures 2c and 2g). Although both Au DENPs

have a similar diameter and crystal structure of the Au core NPs, their absorption features in terms of the surface plasma resonance (SPR) peak are quite different (Figures 2d and 2h): Au-Ac DENPs display an SPR peak at 530 nm, while Au-Gly DENPs at 510 nm. This suggests that different surface modification (acetylation vs hydroxylation) could significantly affect their state of aggregation in aqueous solution.[10, 11] The hydrodynamic size of the Au-Ac DENPs dispersed in water was measured to be 95.6 ± 5.8 nm by DLS, which is almost twice larger than that of the Au-Gly DENPs (50.4 ± 3.2 nm). It is notable that the sizes of both Au DENPs are much larger than those measured by TEM. This could be due to the fact that DLS measures the clustered particles or aggregated particles in aqueous solution that may consist of many single particles, instead TEM measures the single metal core particles in a dry state, in agreement with our previous report.[1] To determine the actual Au loading within the dendrimers, ICP-OES was used and the data show that there are 198 and 193 Au atoms per G5 dendrimer for the Au-Ac DENPs and Au-Gly DENPs, respectively, corroborating the initial Au salt/dendrimer molar ratio (200:1). This indicates that the added Au salt has been completely reduced to Au(0) for both Au DENPs.

Stability Study. The stability of the Au DENPs under different pH and temperature conditions was monitored by UV-vis spectrometry.[1] As shown in Figure S2 (Supporting Information), in the pH range of 4.0-8.0 and under different temperatures (4, 25, 37, and 50 ^{o}C, respectively), the absorption features of both Au DENPs do not display any appreciable changes, suggesting their good stability. Likewise, the hydrodynamic sizes of both Au DENPs do not seem to have a significant change for at least one week. Our results suggest that the PEGylation of dendrimer periphery is an effective approach to generate stable Au DENPs, in agreement with our previous results.[5] Furthermore, the evaluation of the radiostability of the ^{99m}Tc-Au DENPs reveals that no significant degradation of the product can be observed when the particles were exposed to saline or serum up to 6 h (Figure S3, Supporting Information). Taken together, we can conclude that the formed Au DENPs possess good colloidal stability and radiostability.

***In Vivo* Toxicity and Histology Analysis.** Behavior observation, body weight measurement, and

histological changes of the major organs of mice were also used to assess the *in vivo* biosafety of the formed Au DENPs. We show that compared with the control group, mice in the test groups do not present any signs of illness, change in activity, exploratory behavior, eating, and neurological status in a 30-day period. What is more, the two sets of treated mice present similar trends to the control group in the body weight change in the same time period, and there is no notable difference between these three groups (Figure S6, Supporting Information). Furthermore, H&E stained organ slices of both test groups do not show any perceptible lesions, hydropic damages, and any other adverse effect, and the morphology of these organ sections are as normal as that of the control group (Figure S7, Supporting Information).

Serum biochemistry analysis and hematological assessment play the vital role to assess the organ functions. Since the formed materials could be accumulated in liver and spleen (see below *in vivo* biodistribution data), liver function-related blood biochemistry analysis and spleen function-related hematological assessment were carefully performed to reveal any potential toxic effects of the materials. All biochemistry parameters obtained from both tested groups display similar trends to those from the control group (Table S1, Supporting Information). Particularly, the liver function markers including A/G, AST, ALP, and ALT are kept constant in the normal range after injection, indicating the good working order of the liver. Since the excretion is predominantly through urinary system as indicated in SPECT/CT imaging (see below), the BUN level, one of the main indices of renal function, was analyzed to prove the renal safety of the materials. As shown in Table S1, the BUN level of treated mice is as normal as the control mice, suggesting the normal function of kidney. For hematological assessment of the treated mice, the results show that all the five parameters of the test groups are similar to those of the control group, suggesting the good function of spleen (Table S2, Supporting Information). Taken together, both Au DENPs exhibit excellent cytocompatibility and biosafety, which is crucial for their further bioimaging applications.

***In Vivo* Micro-SPECT/CT Imaging.** To quantify the contrast effect, we analyzed the signal intensity of the regions of interest in the SPECT/CT images (Figure S8, Supporting Information).

^{99m}Tc-Au-Ac DENPs show predominant accumulation in lung and bladder, followed by liver and spleen at 0.5 h postinjection (Figure S8a). After that, the signal intensity of lung increases slightly from 0.0048 μCi/mm^3 (0.5 h) to about 0.0055 μCi/mm^3 (1 h), then decreases considerably to 0.0034 μCi/mm^3 (2 h) due to their slow clearance, while that of liver increases slightly from 0.0012 to 0.0023 μCi/mm^3. In contrast, ^{99m}Tc-Au-Gly DENPs show predominant accumulation in blood as indicated by the high signal intensity in heart, kidney, and postcaval vein at 0.5 h postinjection (Figure S8b). Then, the signal intensity of postcaval vein and heart decreases considerably from 0.0030 and 0.0053 μCi/mm^3 (0.5 h) to about 0.00054 and 0.00074 μCi/mm^3 (2 h), respectively, due to their clearance from blood, while that of liver increases slightly from 0.0026 to 0.0041 μCi/mm^3 in the same time frame. For the signal intensity of bladder, both ^{99m}Tc-Au-Ac DENPs and ^{99m}Tc-Au-Gly DENPs are able to be detected at 0.5 h postinjection, indicating their rapid clearance. The signal intensity of bladder remains constant at about 0.003 μCi/mm^3 for ^{99m}Tc-Au-Ac DENPs and 0.004 μCi/mm^3 for ^{99m}Tc-Au-Gly DENPs over 2 h, suggesting that both particles could be excreted out of the body through the urinary system with the time.

To quantify the CT contrast enhancement, the average HU of finely defined regions of interest was measured and the relative HU (RHU) was calculated as the ratio of the HU in the images postinjection and those before injection (Figure S11, Supporting Information). Similarly, the ^{99m}Tc-Au-Ac DENPs show predominant accumulation in lung and bladder, followed by liver and spleen at 0.5 h postinjection. After that, the RHU of lung decreases considerably from 4.7 (0.5 h) to 3.6 (2 h), while that of liver increases slightly from 1.45 to 1.78. In contrast, ^{99m}Tc-Au-Gly DENPs show predominant accumulation in blood as indicated by the high RHU in heart, kidney, and postcaval vein at 0.5 h postinjection. Then, the RHUs of postcaval vein and heart decrease considerably from 5.1 and 2.5 (0.5 h) to about 1.2 and 1.3 (2 h), respectively, due to their clearance from blood, while that of liver increases slightly from 1.9 to 2.6. For the RHU in bladder, both NPs are detectable at 0.5 h postinjection, indicating their rapid clearance. The RHU in the bladder remains constant at 2.5 for the ^{99m}Tc-Au-Ac DENPs and 3.0 for the ^{99m}Tc-Au-Gly DENPs, respectively over the period of 2 h,

indicating that the Au DENPs are able to be filtered *via* kidney and go into the bladder. These results are consistent with those obtained from SPECT imaging. Taken together with SPECT and CT imaging results, we can conclude that the developed ^{99m}Tc-labeled Au DENPs are able to be used as a dual mode contrast agent for SPECT/CT imaging applications.

***In Vivo* Biodistribution.** To further investigate the *in vivo* biodistribution behavior of the ^{99m}Tc-labeled Au DENPs, post-mortem γ-scintigraphy was conducted in parallel to SPECT/CT imaging. As shown in Figure S12a (Supporting Information), the results correlate well with the SPECT images: the lung, liver, and spleen are the major organs accumulated with the ^{99m}Tc-Au-Ac DENPs, while other organs such as heart, kidney, blood, muscle, and brain have the relatively low uptake of the particles (the percentage of injection dose per gram tissue, %ID/g). In view of the organ biodistribution over time, the uptake of ^{99m}Tc-Au-Ac DENPs seem to decrease in lung significantly (from 14% to 0.6% ID/g) and increase in liver and spleen (from 5.8% and 1.5% to 11% and 4.5% ID/g, respectively) within 12 h postinjection. On the contrary, a markedly different organ biodistribution profile was observed for the ^{99m}Tc-Au-Gly DENPs (Figure S12b). It is clear that the uptake of the particles in blood (3.0% ID/g) at 1 h postinjection gradually decreases and remains 1.4%, 1.1%, and 0.53% ID/g at 2, 4, and 12 h postinjection, respectively. Meanwhile, similar to that of blood, the ^{99m}Tc content of heart is relatively high in the first 4 h and continuously decreases with the time. It is noteworthy that kidney have the highest ^{99m}Tc content (5.0% ID/g) at 1 h post injection among the organs listed, which means that the excretion of particles is predominantly through urinary system, similar to the SPECT/CT imaging results. With the time postinjection, the particles are able to be cleared from blood and taken up by the liver and spleen and the content of ^{99m}Tc in liver and spleen increases consistently from 2.9% and 3.1% to 9.4% and 7.4% ID/g at 12 h postinjection, respectively. At all the time points, the ^{99m}Tc content at lung, muscle and brain is relatively low.

To determine the long term *in vivo* biodistribution of the Au DENPs without ^{99m}Tc labeling, ICP-OES analysis was used to evaluate the Au content within the heart, liver, spleen, lung, and kidney at 48, 96, and 168 h postinjection (Figure S13, Supporting Information). As expected, the largest

fractions of Au were observed in the liver and spleen for both Au DENPs and their content shows a marked reduction with the time postinjection. It is notable that most of the Au DENPs are able to be cleared from the body at 168 h post administration.

References:

1. S. Wen, K. Li, H. Cai, Q. Chen, M. Shen, Y. Huang, C. Peng, W. Hou, M. Zhu, G. Zhang and X. Shi, *Biomaterials*, 2013, **34**, 1570-1580.
2. M. Motaleb, *J. Radioanal. Nucl. Chem.*, 2007, **272**, 95-99.
3. H. Cai, X. An, J. Cui, J. Li, S. Wen, K. Li, M. Shen, L. Zheng, G. Zhang and X. Shi, *ACS Appl. Mater. Interfaces*, 2013, **5**, 1722-1731.
4. J. V. Jokerst, T. Lobovkina, R. N. Zare and S. S. Gambhir, *Nanomedicine*, 2011, **6**, 715-728.
5. C. Peng, L. Zheng, Q. Chen, M. Shen, R. Guo, H. Wang, X. Cao, G. Zhang and X. Shi, *Biomaterials*, 2012, **33**, 1107-1119.
6. M. Roberts, M. Bentley and J. Harris, *Adv. Drug Delivery Rev.*, 2012, **64**, 116-127.
7. S. Zhu, M. Hong, G. Tang, L. Qian, J. Lin, Y. Jiang and Y. Pei, *Biomaterials*, 2010, **31**, 1360-1371.
8. X. Y. Shi, I. Banyai, M. T. Islam, W. Lesniak, D. Z. Davis, J. R. Baker and L. P. Balogh, *Polymer*, 2005, **46**, 3022-3034.
9. X. Y. Shi, W. Lesniak, M. T. Islam, M. C. Muniz, L. P. Balogh and J. R. Baker, *Colloids Surf., A*, 2006, **272**, 139-150.
10. D. Liu, Z. Wang and X. Jiang, *Nanoscale*, 2011, **3**, 1421-1433.
11. S. K. Ghosh and T. Pal, *Chem. Rev.*, 2007, **107**, 4797-4862.

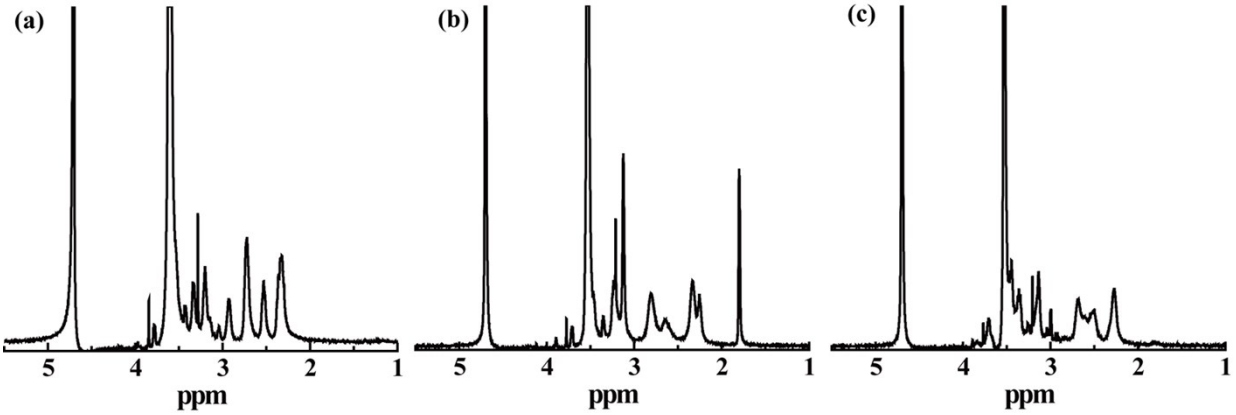

Figure S1. ^{1}H NMR spectra of G5-DTPA-*m*PEG (a), Au-Ac DENPs (b), and Au-Gly DENPs (c) dissolved in D_2O.

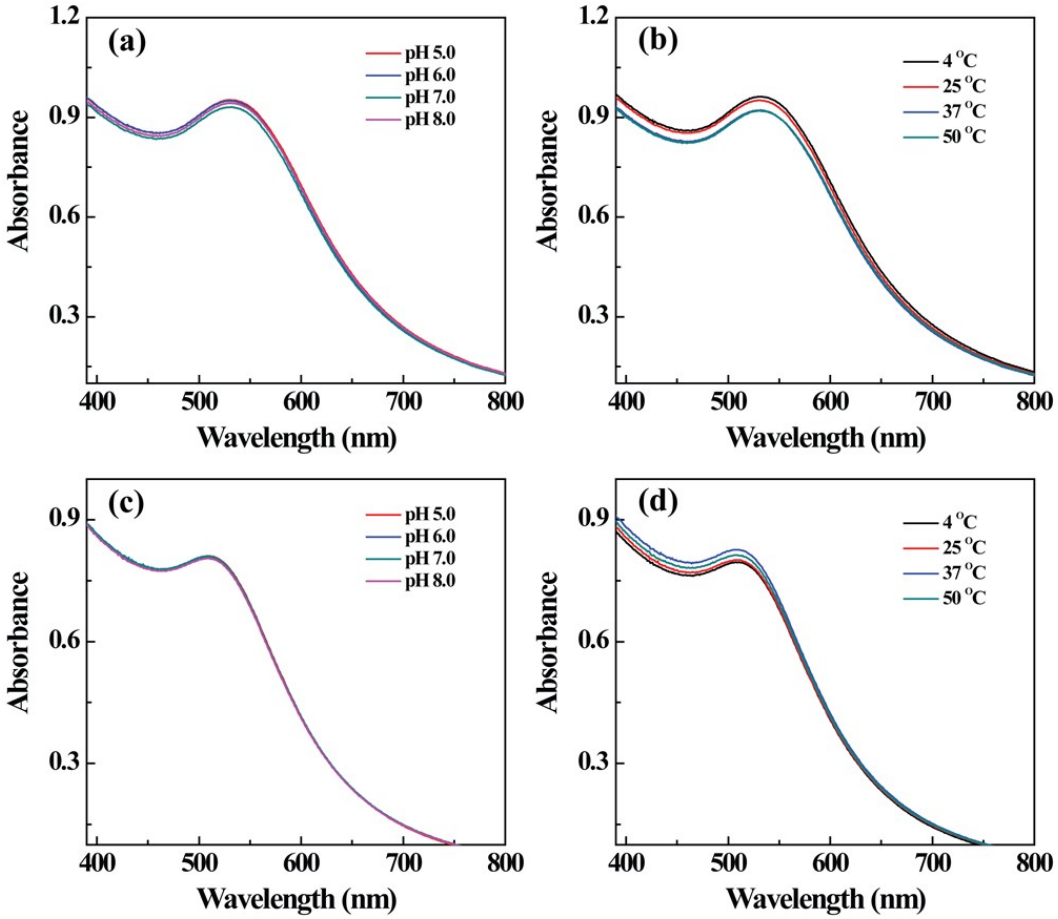

Figure S2. UV-vis spectra of Au-Ac DENPs (a, b) and Au-Gly DENPs (c, d) under different pH (a, c) and temperature (b, d) conditions.

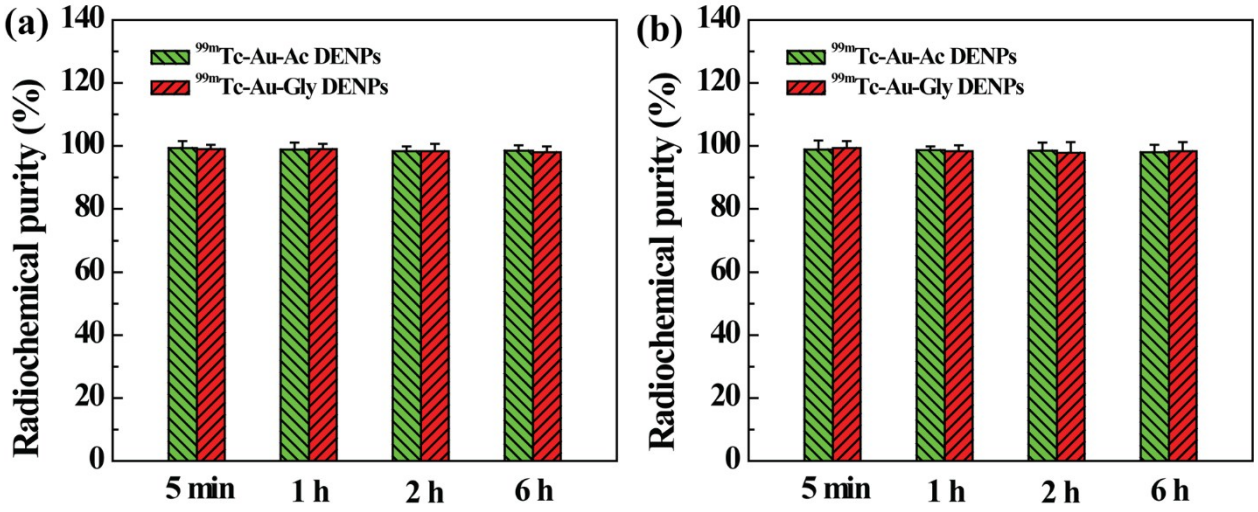

Figure S3. Radiochemical stability of the ^{99m}Tc-Au-Ac DENPs and ^{99m}Tc-Au-Gly DENPs incubated in saline (a) and serum (b) for different time periods.

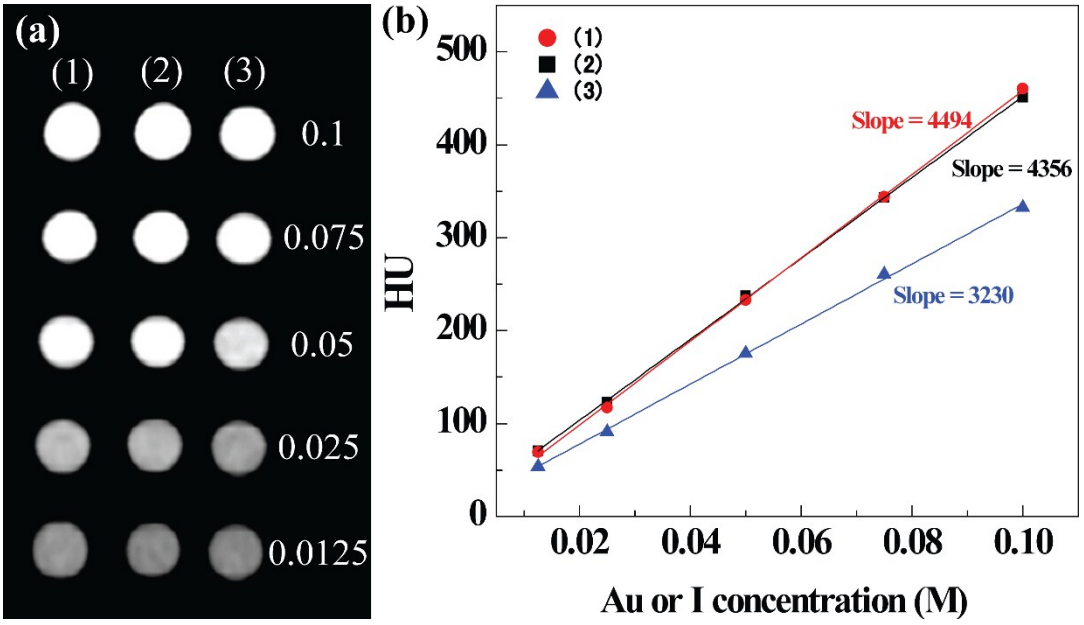

Figure S4. CT phantom images (a) and X-ray attenuation (HU) (b) of the Au-Gly DENPs (1), Au-Ac DENPs (2) and Omnipaque (3) as a function of Au or I concentration.

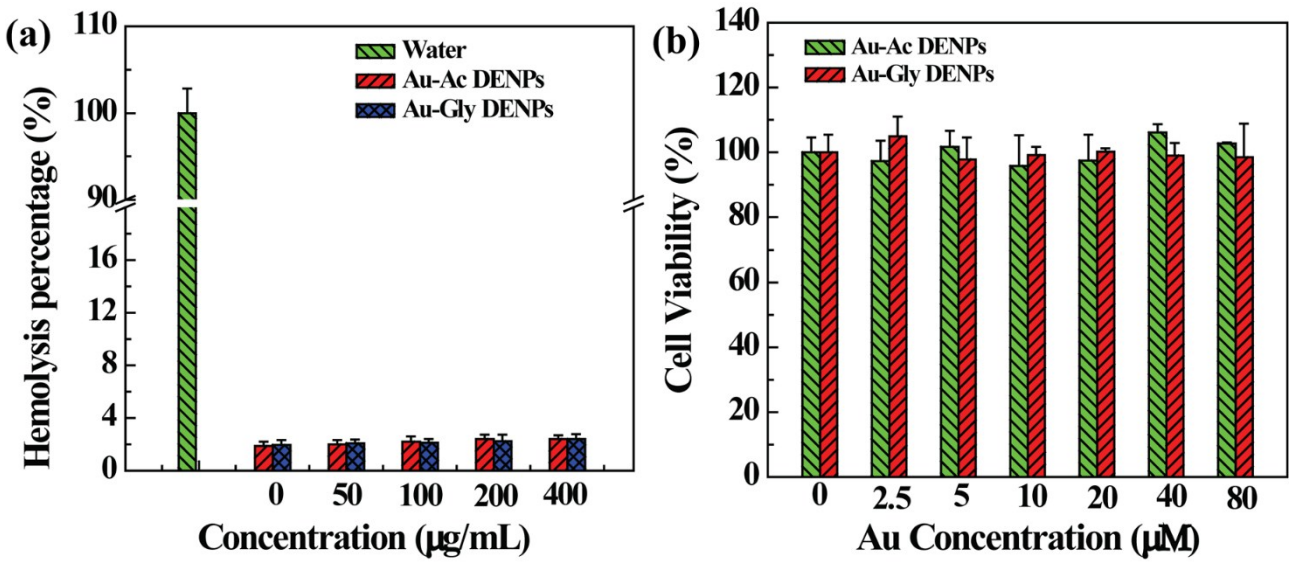

Figure S5. (a) Hemolytical activity of the Au-Ac DENPs and Au-Gly DENPs at different concentrations. (b) MTT assay of the viability of SKOV-3 cells after treatment with Au-Ac DENPs and Au-Gly DENPs at different Au concentrations for 24 h.

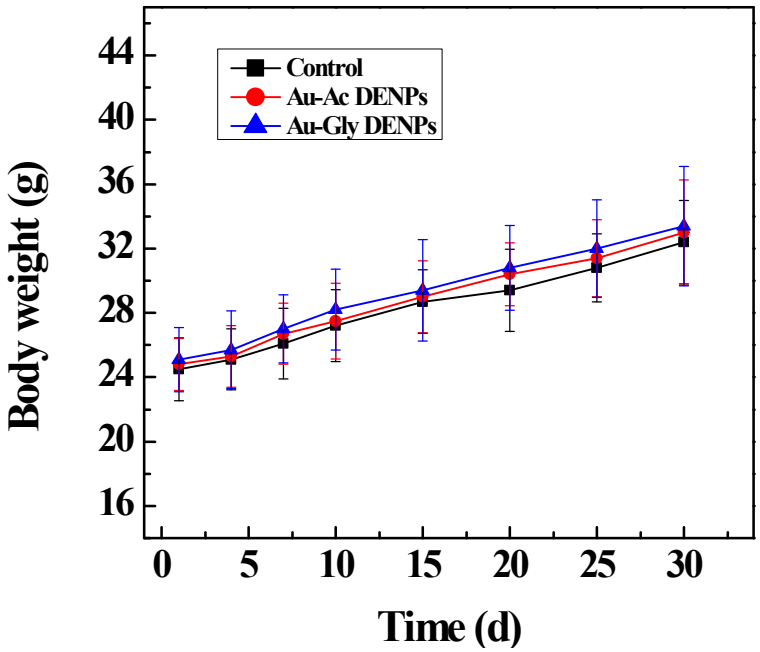

Figure S6. Changes in body weight obtained from mice injected with the Au-Ac DENPs or Au-Gly DENPs. Mice injected with saline were used as control.

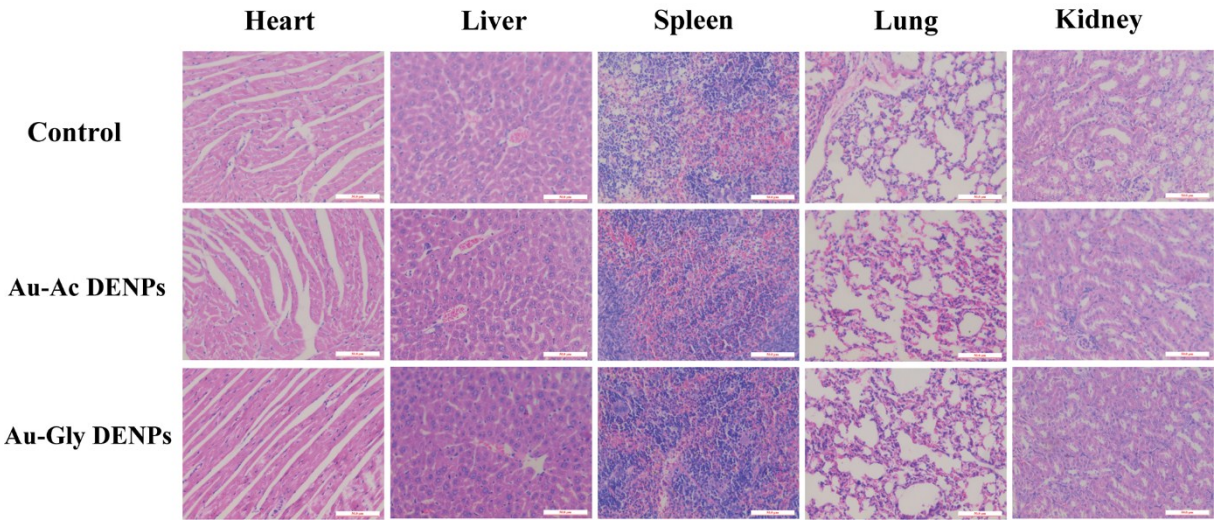

Figure S7. Histological changes of the mouse organs stained with H&E at 30 days post administration of the Au-Ac DENPs or Au-Gly DENPs. The scale bar in each panel represents 50 μm.

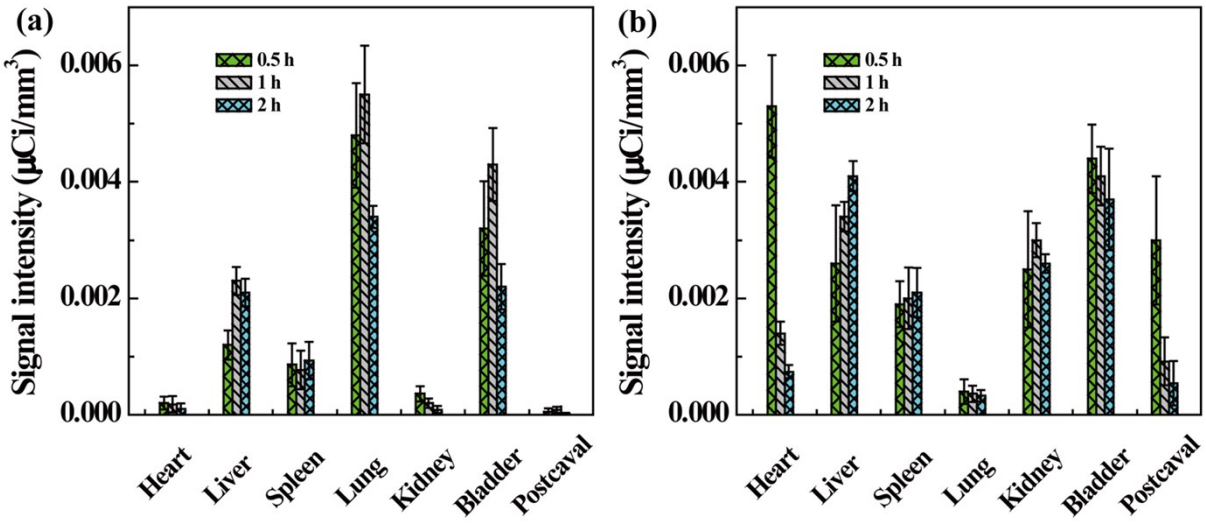

Figure S8. SPECT signal intensity of different organs at different time points postinjection of the ^{99m}Tc-Au-Ac DENPs (a) and ^{99m}Tc-Au-Gly DENPs (b).

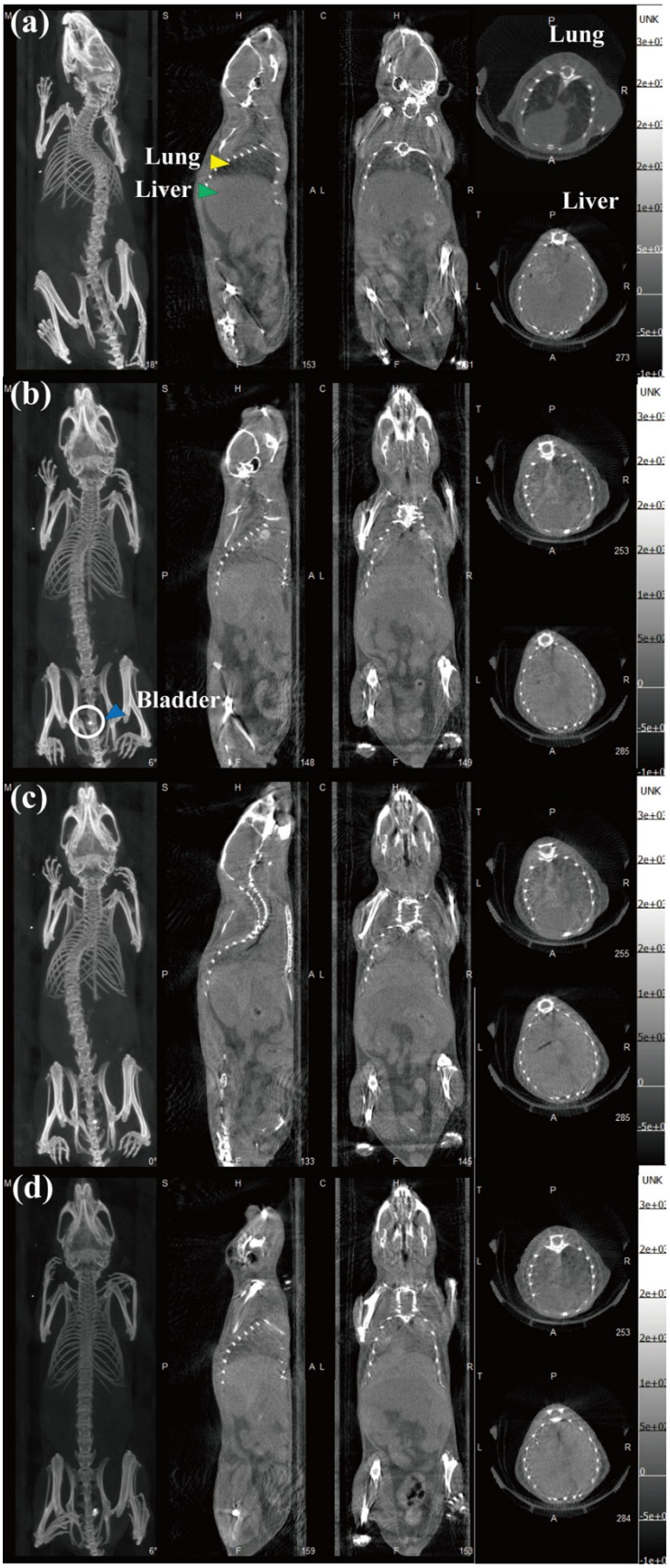

Figure S9. Micro-CT images of a mouse lung, liver, and bladder before (a) and at 0.5 h (b), 1 h (c), and 2 h (d) postinjection of the ^{99m}Tc-Au-Ac DENPs.

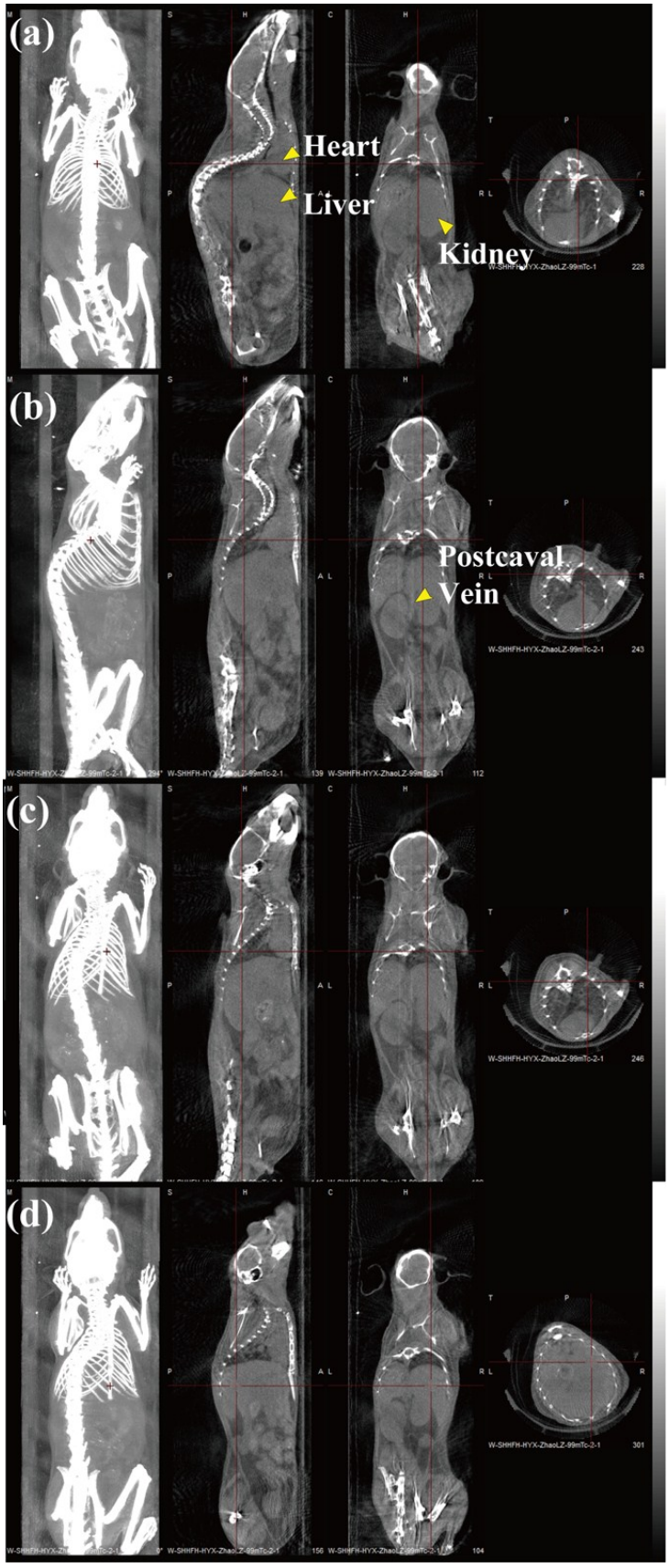

Figure S10. Micro-CT images of a mouse heart, liver, kidney and postcaval vein before (a) and at 0.5 h (b), 1 h (c), and 2 h (d) postinjection of the ^{99m}Tc-Au-Gly DENPs.

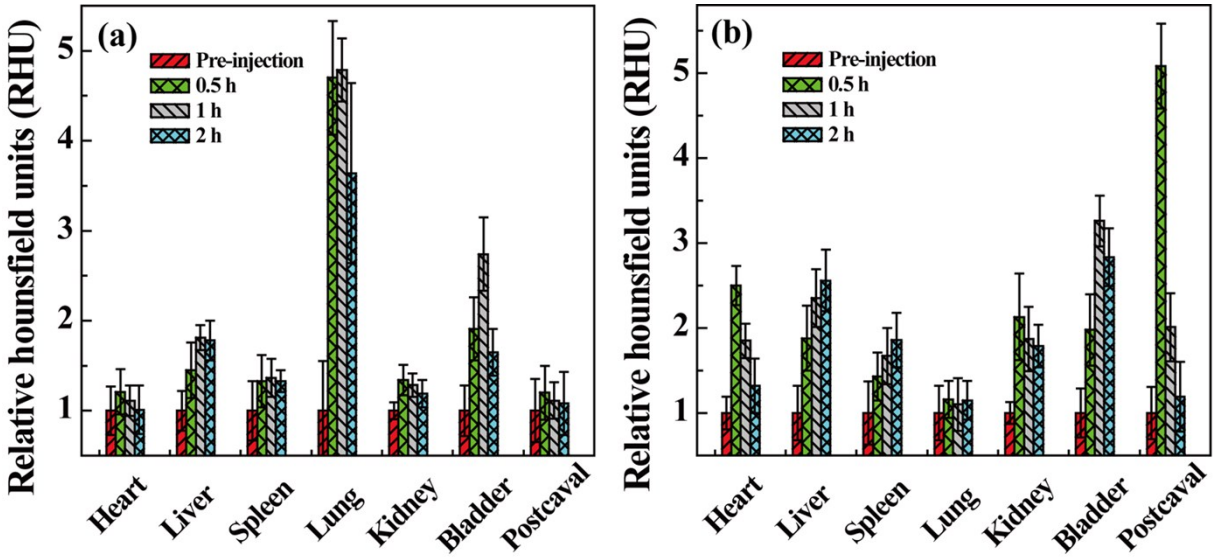

Figure S11. Relative CT value of different organs before and at different time points postinjection of the ^{99m}Tc-Au-Ac DENPs (a) and ^{99m}Tc-Au-Gly DENPs (b).

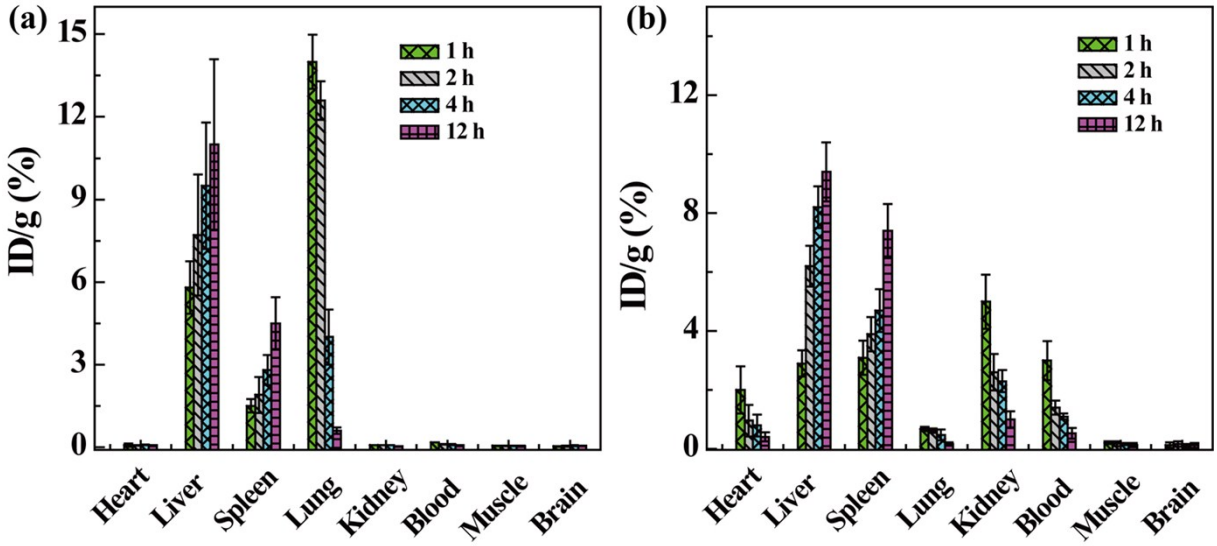

Figure S12. Biodistribution of ^{99m}Tc in the blood, muscle, and major organs of the mice at different time points postinjection of the ^{99m}Tc-Au-Ac DENPs (a) and ^{99m}Tc-Au-Gly DENPs (b).

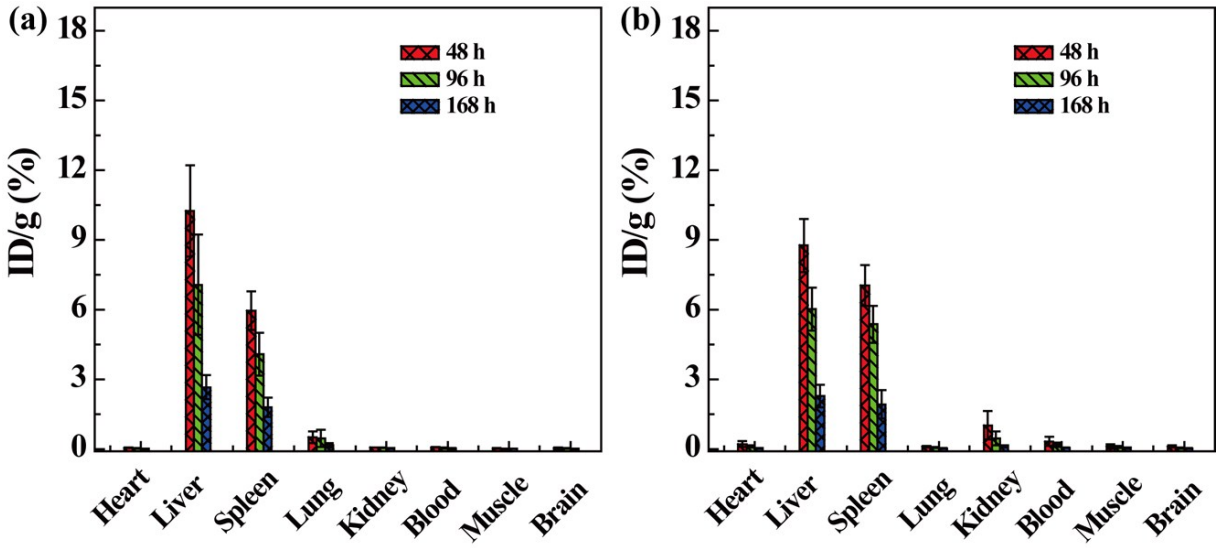

Figure S13. Biodistribution of Au in the blood, muscle, and major organs of the mice at different time points postinjection of the Au-Ac DENPs (a) and Au-Gly DENPs (b).

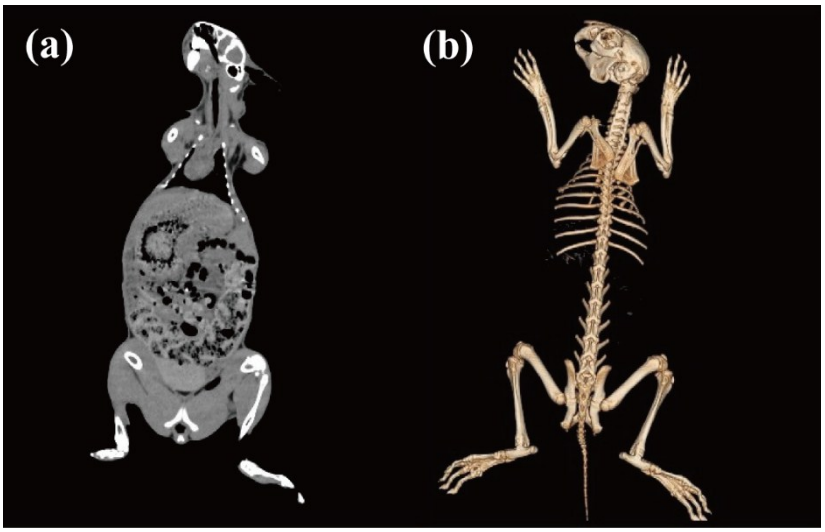

Figure S14. CT image (a) and corresponding 3D renderings of CT image (b) of a rabbit before hock injection of the ^{99m}Tc-Au-Ac DENPs (left paw) and ^{99m}Tc-Au-Gly DENPs (right paw).

Table S1. Serum biochemistry parameters of mice at 30 days postinjection of saline, Au-Ac DENPs, and Au-Gly DENPs.

	ALP (U/L)	A/G	AST (U/L)	ALT (U/L)	BUN (mM)
Saline	158 ± 21	0.73 ± 0.14	145 ± 22	56 ± 8.5	8.2 ± 1.9
Au-Ac DENPs	169 ± 26	0.67 ± 0.12	154 ± 13	50 ± 10	7.8 ± 1.6
Au-Gly DENPs	156 ± 19	0.78 ± 0.18	141 ± 19	53 ± 6	8.4 ± 2.3

Table S2. Hematology parameters of mice at 30 days postinjection of saline, Au-Ac DENPs, and Au-Gly DENPs.

	WBC (10^9/L)	RBC (10^{12}/L)	HGB (g/L)	HCT (L/L)	PLT (10^{12}/L)
Saline	8.5 ± 2.0	10.6 ± 1.6	166 ± 31	0.68 ± 0.15	1.55 ± 0.27
Au-Ac DENPs	7.9 ± 1.8	11.1 ± 2.3	157 ± 24	0.73 ± 0.12	1.62 ± 0.19
Au-Gly DENPs	8.1 ± 2.5	10.8 ± 1.9	169 ± 27	0.64 ± 0.09	1.49 ± 0.22